Proc. Natl. Acad. Sci. USA
Vol. 89, pp. 4786–4790, June 1992
Biochemistry

Definition of the catalytic site of cytochrome *c* oxidase: Specific ligands of heme *a* and the heme a_3–Cu_B center

JAMES P. SHAPLEIGH*, JONATHAN P. HOSLER†, MARY M. J. TECKLENBURG‡§, YOUNKYOO KIM‡, GERALD T. BABCOCK‡, ROBERT B. GENNIS*, AND SHELAGH FERGUSON-MILLER†

*School of Chemical Sciences, University of Illinois, Urbana, IL 61801; and Departments of †Biochemistry and ‡Chemistry, Michigan State University, East Lansing, MI 48824

Communicated by N. Edward Tolbert, February 6, 1992 (received for review November 17, 1991)

ABSTRACT **The three-subunit aa_3-type cytochrome *c* oxidase (EC 1.9.3.1) of *Rhodobacter sphaeroides* is structurally and functionally homologous to the more complex mitochondrial oxidase. The largest subunit, subunit I, is highly conserved and predicted to contain 12 transmembrane segments that provide all the ligands for three of the four metal centers: heme *a*, heme a_3, and Cu_B. A variety of spectroscopic techniques identify these ligands as histidines. We have used site-directed mutagenesis to change all the conserved histidines within subunit I of cytochrome *c* oxidase from *Rb. sphaeroides*. Analysis of the membrane-bound and purified mutant proteins by optical absorption and resonance Raman spectroscopy indicates that His-102 and His-421 are the ligands of heme *a*, while His-284, His-333, His-334, and His-419 ligate the heme a_3–Cu_B center. To satisfy this ligation assignment, helices II, VI, VII, and X, which contain these histidine residues, must be in close proximity. These data provide empirical evidence regarding the three-dimensional protein structure at the catalytic core of cytochrome *c* oxidase.**

Cytochrome *c* oxidase (EC 1.9.3.1) catalyzes the reduction of oxygen to water at the terminus of the mitochondrial respiratory chain, the principal energy-generating system of eukaryotic organisms (for recent reviews see refs. 1 and 2). Energy conservation is achieved by the coupling of electron transfer through the heme and copper metal centers to proton translocation across the membrane (3). To understand this coupling process it is essential to have a detailed description of the protein structures that form the heme- and copper-binding sites.

A number of bacteria synthesize cytochrome *c* oxidases that are simpler in structure but functionally homologous to the mitochondrial enzymes (2, 4, 5). The aa_3-type cytochrome *c* oxidase from *Rhodobacter sphaeroides* has recently been purified as a complex of three subunits that are homologues of the three mitochondrially encoded subunits of the eukaryotic oxidase (J.P.H. and S.F.-M., unpublished results). The *Rb. sphaeroides* oxidase has remarkably high turnover ($V_{max} > 1800\ sec^{-1}$), pumps protons efficiently (0.7 H^+/e^-) in reconstituted proteoliposomes, and is spectroscopically similar to beef heart cytochrome *c* oxidase. This preparation clearly establishes the oxidase from *Rb. sphaeroides* as an excellent bacterial model for examining the structural basis of the catalytic function of the more complex eukaryotic enzyme. The utility of *Rb. sphaeroides* as a genetic system for analyzing structure/function relationships has been established in previous studies of the photosynthetic reaction center (6) and the cytochrome bc_1 complex (7).

The genes coding for the three subunits of the *Rb. sphaeroides* aa_3-type oxidase have been cloned and sequenced (refs. 8 and 9 and unpublished data). The genetic organization and deduced amino acid sequences are very similar to those from the closely related bacterium *Paracoccus denitrificans* (2, 10–12). In addition, subunit I shows 50% sequence identity to subunit I of bovine heart cytochrome *c* oxidase (9).

Hydropathy profile analysis of subunit I from *Rb. sphaeroides* is consistent with 12 transmembrane helical spans, as previously proposed for bovine subunit I (11). The two-dimensional model that emerges from this analysis (Fig. 1) highlights seven histidine residues, six of which are found to be totally conserved (His-102, His-284, His-333, His-334, His-419, and His-421), while the seventh (His-411) is absent only in the sequence from *Bradyrhizobium japonicum* (13, 14), in an alignment of amino acid sequences of subunit I from various species. Spectroscopic studies of bovine heart cytochrome *c* oxidase have shown that heme *a* is ligated by two histidine residues (15–18), heme a_3 by a single histidine (19, 20), and Cu_B by at least three histidines (21, 22). Since the histidines that are metal ligands will almost certainly be conserved throughout the entire family of oxidases, the set of six totally conserved histidines found in subunit I should coincide with the six histidines defined as metal ligands by physical methods. To test this postulate, and to establish the assignments of the particular ligands of heme *a*, heme a_3, and Cu_B, we have prepared and analyzed site-directed mutants of the conserved histidines. Our results define the two histidines that ligate heme *a* and the four histidines that ligate the heme a_3–Cu_B (binuclear) center. A model of the protein structure surrounding these three metal centers is presented.

METHODS

Site-Directed Mutagenesis. The construction of the initial vector, pJS1, containing the *ctaD* (*coxI*) gene of *Rb. sphaeroides* is described elsewhere (9). To facilitate mutagenesis, an *Xba* I and a *Kpn* I site were introduced by site-directed mutagenesis at nucleotides 204 and 675 of the *ctaD* open reading frame. These changes do not alter the primary sequence of subunit I. This new vector was designated pJS3. To mutate His-102, a 473-base-pair (bp) *Xba* I–*Kpn* I fragment of *ctaD* from pJS3 was inserted into the phagemid pT7T3-18U (Pharmacia). To mutate His-284, His-333, and His-334, a 455-bp *Kpn* I–*Sst* I fragment of *ctaD* was inserted into the phagemid pT7T3-18U. After mutagenesis, these mutants were inserted back into pJS3 by using a *Kpn* I–*Bgl* II fragment, since the *Sst* I site is not unique. A 220-bp *Sal* I–*Sph* I fragment was inserted into pT7T3-19U (Pharmacia) to mutate His-411, His-419, and His-421. To reintroduce this fragment back into *ctaD* it was initially inserted into a *Bam*HI–*Hin*dIII fragment of pJS3, and then a *Bgl* II–*Hin*dIII fragment of this construct was inserted into pJS3. This was necessary because the *Sal* I site is not unique.

Mutagenesis was carried out by the method of Vandeyar *et al.* (23) on single-stranded DNA produced from the

The publication costs of this article were defrayed in part by page charge payment. This article must therefore be hereby marked "*advertisement*" in accordance with 18 U.S.C. §1734 solely to indicate this fact.

§Present address: Department of Chemistry, Central Michigan University, Mt. Pleasant, MI 48859.

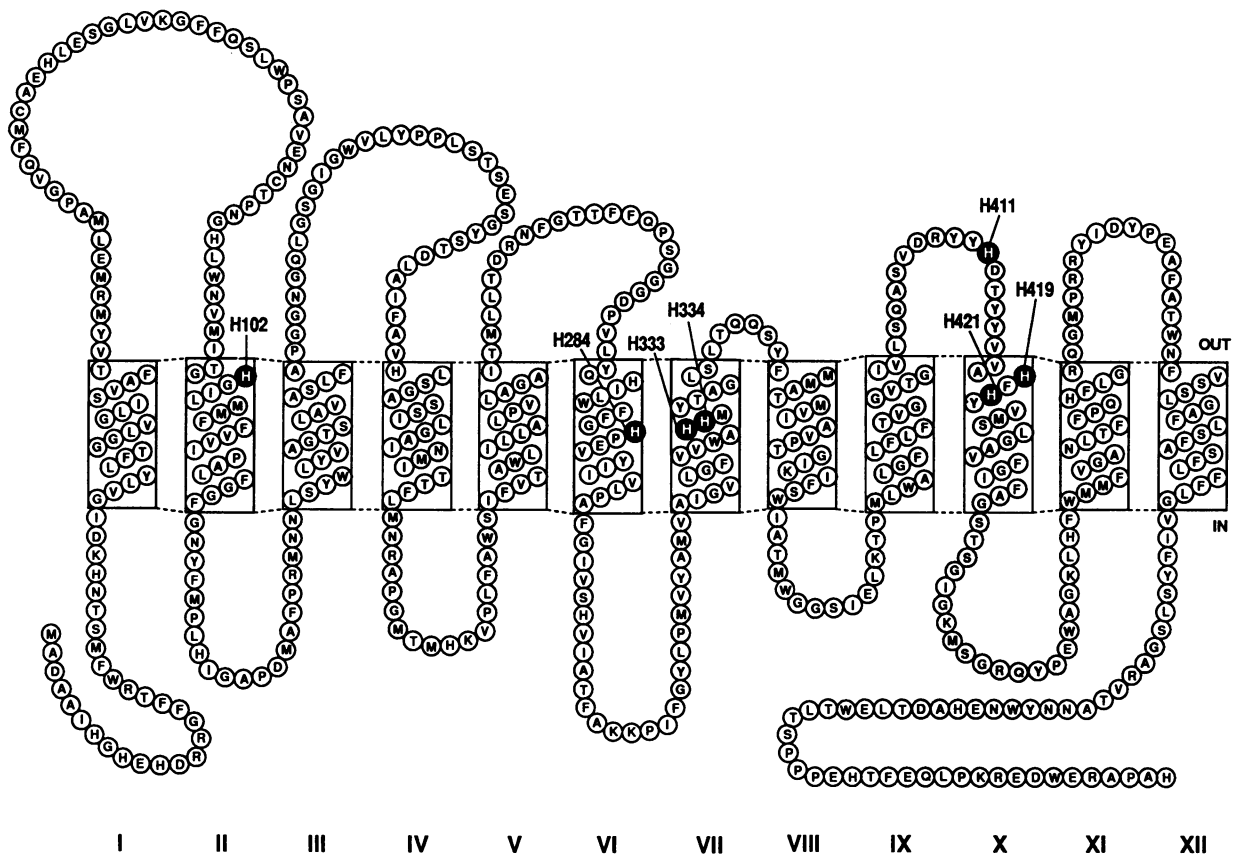

FIG. 1. Amino acid sequence of subunit I of *Rb. sphaeroides* cytochrome *c* oxidase, showing 12 predicted transmembrane helices. The seven histidines that are the focus of this study are highlighted.

phagemids. Synthetic oligonucleotides 18–21 bases long containing one or two mismatches were used to mutagenize the histidine codons. All mutations were verified by sequencing using the dideoxy chain-termination method (24).

Mutant sequences were inserted back into pJS3 and then the entire insert was cloned in pRK415-1 (25). These constructs were used to transform *Escherichia coli* S17-1 (26) and were conjugated into *Rb. sphaeroides* JS100, a strain in which the region of *ctaD* coding for the conserved histidines has been deleted by gene replacement (9). Mutants and wild type strains were grown in Sistrom's medium (27). In the case of mutants, antibiotics were added: streptomycin (50 μg/ml), spectinomycin (50 μg/ml), and tetracycline (1 μg/ml).

Oxidase Purification. The native and mutant versions of cytochrome aa_3 were purified by solubilization of bacterial cytoplasmic membranes with lauryl maltoside followed by chromatography on hydroxyapatite and DEAE-5PW (Tosoh, Tokyo). Details of the purification procedure will be published elsewhere.

Spectroscopic Methods. Optical spectra were recorded with a Perkin–Elmer Lambda 6 UV/visible spectrophotometer at 25°C. Pyridine hemochromogen spectra of the purified His-333 → Asn mutant were obtained from dithionite-reduced samples containing 0.5 μM oxidase, 0.2 M NaOH, and 10% (vol/vol) pyridine (28).

Resonance Raman spectra were obtained by using Spex 1401 and 1877 spectrometers with photomultiplier and photodiode array detectors, respectively. Excitation at 441.6 nm was provided by a Liconix HeCd laser that was operated at 10 mW power. Cytochrome *c* oxidase (35 μM), in 100 mM KH_2PO_4, pH 7.6/1 mM EDTA/0.5% lauryl maltoside, was reduced with sodium dithionite and placed in capillary tubes for spectra acquisition. The temperature was maintained between 1°C and 7°C by using cold N_2 gas. Optical spectra were recorded before and after the Raman experiments to ensure sample integrity and reduction.

RESULTS

Membrane-Bound Mutants: Visible Spectra. Fig. 2 shows the reduced-minus-oxidized visible absorption spectra of cytoplasmic membranes isolated from eight different mutants as well as from the wild-type control. The α-band (605–607 nm) associated with heme *a* (29) is present in all cases, except for two mutants, His-102 → Asn and His-421 → Asn. Immunoblots (not shown) indicate that subunit I is present in all cases, including the two mutants that lack heme *a* spectroscopically. These data provide the initial suggestive evidence that His-102 and His-421, in helices II and X, are the two axial ligands to heme *a*. All of the other mutants retain the α-band ascribed to heme *a*, but the wavelength maximum for that peak is shifted by 1–2 nm compared to wild type. This indicates a subtle change in the environment of heme *a* due to each of these mutations.

Purified Mutants: Characteristics. Further spectroscopic and enzymological analysis of the mutant oxidases required that they be purified. This was necessary because of the relatively low level of expression of some of the mutant aa_3-type oxidases, as well the presence of a second cytochrome *c* oxidase, a *co*-type, present in the membranes of *Rb. sphaeroides*. With the exception of mutants with altered His-102 or His-421, the mutant enzymes could all be substantially purified without significant change of their absorbance spectra, including the slight blue shift of the α-band. The His-102 → Asn and His-421 → Asn mutants could not be purified. These heme *a*-deficient species appear to be denatured during the purification procedures, as might be expected if heme *a* normally stabilizes an association between helices II

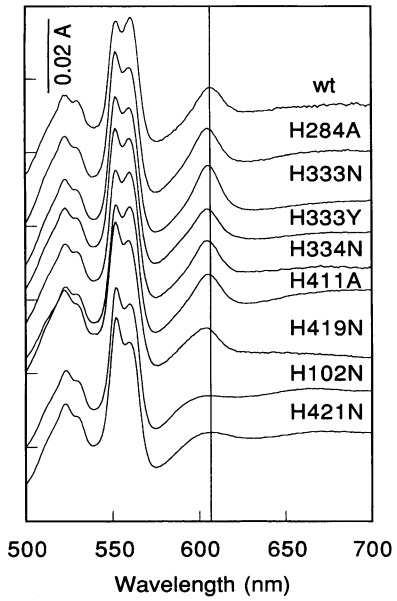

FIG. 2. Dithionite-reduced minus ferricyanide-oxidized visible spectra of cytoplasmic membranes of wild type (wt, strain 2.4.1) and of a set of histidine mutants in subunit I of *Rb. sphaeroides* cytochrome *c* oxidase. H284A = His-284 → Ala, etc.

and X that is critical for establishing the overall three-dimensional structure and subunit assembly (see ref. 30).

Table 1 summarizes the results obtained from studies of six purified mutant oxidases, not including His-102 → Asn and His-421 → Asn, which could not be characterized because of their instability to purification. The modified proteins were analyzed in terms of their heme *a* and a_3 content by visible spectroscopy, their CO binding, and their oxygen reduction activity. All of the mutants contain both hemes but are altered in CO binding and are devoid of cytochrome *c* oxidase activity, except for the His-411 → Ala mutant, which appears essentially native in all these respects. This mutant also retains the ability to pump protons (31). From these results, it is apparent that His-411, which is placed outside of the lipid bilayer in the two-dimensional model of subunit I (Fig. 1), is not a redox center ligand and is not required for oxidase activity. This finding requires a revision of previous models of cytochrome *c* oxidase in which this histidine is proposed to be a ligand for heme *a* (2, 11).

Purified Mutants: Resonance Raman Analysis. To further examine the effect of each of the histidine substitutions on the structure of the oxidase, resonance Raman spectroscopy was utilized. This technique is particularly powerful for probing the influence of the protein environment on each of the heme centers of cytochrome oxidase (32). Purified samples of oxidase are required for these experiments and, hence, the His-102 and His-421 mutants could not be examined.

Resonance Raman spectra of the mutant oxidase species (Fig. 3) show that amino acid substitutions for the histidines at positions 284, 333, 334, 411, or 419 do not alter the normal heme *a* vibrational modes at 1610 cm^{-1} (formyl stretch) or 1624 cm^{-1} (vinyl stretch) (32). It is highly unlikely that the loss of bis(histidine) ligation of heme *a* would leave unperturbed these modes as well as the visible absorption band associated with this heme (Fig. 2 and Table 1). Thus, His-284, His-333, His-334, His-411, and His-419 can be ruled out as axial ligands to heme *a*. Therefore, heme *a* must be ligated to His-102 in helix II and His-421 in helix X. Since His-411 is not an essential residue, the remaining four conserved histidines (284, 333, 334, and 419) can be assigned as ligands to the binuclear center. Indeed, vibrational modes associated with heme a_3, 1662, 365 and 214 cm^{-1}, are altered in mutants of these residues (Fig. 3 and see *Discussion*).

DISCUSSION

It might be expected that substitution of the axial ligand to heme a_3 would eliminate this heme component from the oxidase. However, the absorbance spectra and pyridine hemochromogen analysis of the purified oxidase mutants indicate that this is not the case. Since all the mutants at positions 284, 333, 334, and 419 have similar optical properties (Table 1), it is concluded that in all cases heme a_3 is present, albeit in an altered environment.

Presumably, one of these four conserved histidines (284, 333, 334, or 419) is the axial ligand to heme a_3 in the native enzyme. Therefore, ligand substitution must be invoked to explain the presence of this heme in the binuclear center when the proximal histidine is replaced by mutagenesis. Ligand switching has in fact been observed in a hemoglobin mutant lacking the proximal histidine (36): crystallographic analysis shows that the distal histidine is bound to the heme iron, taking over the function of the altered proximal ligand. In the case of cytochrome oxidase, one of the nearby copper ligands (e.g., His-419) might be recruited to bind the iron of heme a_3.

The mutations at positions 284, 333, 334, and 419 each cause a diminution in the binding of CO to the heme a_3–Cu_B center, as measured by the perturbation of the visible spectrum (Table 1). The loss of CO binding is most dramatic for the His-284 → Ala and His-419 → Asn mutants, indicating an

Table 1. Comparison of the spectroscopic and catalytic properties of purified mutant and wild-type cytochrome *c* oxidases from *Rb. sphaeroides*

Property	Wild type	His-284 → Ala	His-333 → Asn	His-333 → Tyr	His-334 → Asn	His-411 → Ala	His-419 → Asn
Presence of heme *a**	+	+	+	+	+	+	+
Presence of heme a_3†	+	+	+	+	+	+	+
α-Band absorbance maximum, nm	605.5	604.5	604.5	604	604	604.5	604
CO binding, % of wild type	100	16–76	57	45	46	100	20–40
Cytochrome c oxidase activity‡, % of wild type	100	0	0	0	0	80	0

This table does not include His-102 → Asn and His-421 → Asn because they have lost the α-band, which allows investigation of the enzyme in the intact membrane, and they are unstable to purification, as discussed in the text.

*From α-band intensity (Fig. 2) and resonance Raman spectra (Fig. 3).

†From the ratio of the absorbance in the Soret band (442–444 nm) relative to the intensity of the α-band. This value is 5.5 for wild-type oxidase and His-411 → Ala, but it decreases to approximately 4.8 for all of the other mutant oxidases, apparently due to a lower extinction coefficient for heme a_3 in these altered proteins, since pyridine hemochromagen analysis indicates similar heme content.

‡Oxygen reduction activity is measured polarographically in a reaction containing 50 mM KH_2PO_4 at pH 6.5, 1 mM lauryl maltoside, 2.8 mM ascorbate, 0.55 mM *N,N,N',N'*-tetramethyl-*p*-phenylenediamine, 30 μM horse-heart cytochrome *c*, and 4–10 pmol of oxidase. The activity of the wild-type control was 1600 sec^{-1}.

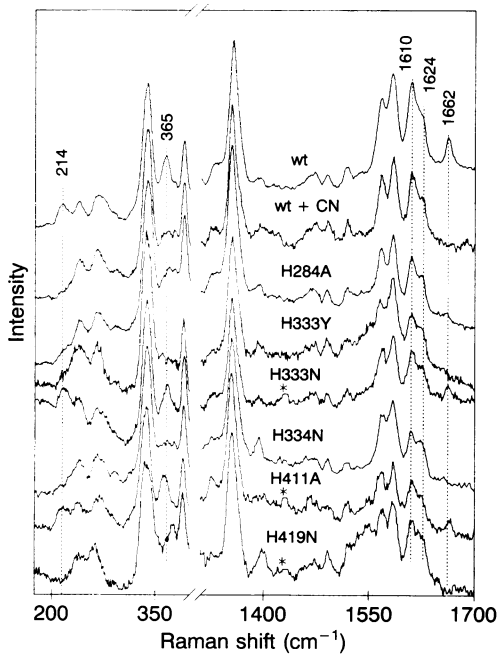

FIG. 3. Resonance Raman spectra of fully reduced cytochrome *c* oxidase purified from wild type and mutants of *Rb. sphaeroides*. With cyanide bound to the mixed-valence enzyme (a^{2+} a_3^{3+}–CN^-; wt + CN^-) only those signals due to heme *a* are present (32). Indicated in the figure are the formyl (1610 cm^{-1}) and vinyl (1624 cm^{-1}) stretches of heme *a* and the formyl stretch (1662 cm^{-1}), the ring bending mode (365 cm^{-1}), and the Fe–N_{His} stretch (214 cm^{-1}) of heme a_3. The spectrum of the wild-type bacterial oxidase is remarkably similar to that of bovine heart cytochrome *c* oxidase (32–35), with the notable exception of an increased intensity of the heme *a* formyl mode at 1610 cm^{-1}. The asterisks indicate the position of the peak due to excess dithionite (deleted).

altered environment of the binuclear center. The fact that the amount of CO bound to the His-284 → Ala and His-419 → Asn mutants can be substantially increased by manipulation of the temperature or the time of exposure to CO strongly suggests that access to heme a_3 is limited by altered protein conformation in this region. Again, the simplest conclusion is that each of these mutations significantly alters the binuclear center, even though heme a_3 is retained.

Resonance Raman spectra (Fig. 3) show that the three modes known to result from heme a_3 interactions with the protein, the formyl stretch at 1662 cm^{-1}, the ring bending mode at 365 cm^{-1}, and the Fe–N_{His} stretch at 214 cm^{-1} (32), are present only in the native enzyme, His-411 → Ala, and His-333 → Asn. In the other four purified mutants (His-284 → Ala, His-333 → Tyr, His-334 → Asn, and His-419 → Asn) these bands are absent.

The presence of the heme a_3-specific bands in the His-333 → Asn mutant rules out His-333 as the axial ligand to heme a_3, since replacement of the proximal histidine by asparagine should cause detectable changes in these resonance Raman features. Indeed, the replacement of His-333 by tyrosine does eliminate the heme a_3-specific resonance Raman bands. Based on the His-333 → Asn result, this cannot be a direct effect on heme a_3 and must rather be due to conformational changes in the protein pocket containing the binuclear center. Since the amino acid substitutions for His-284, His-334, and His-419 also eliminate these heme a_3-specific resonance Raman bands, the data are consistent with the assignment of these four conserved histidines (284, 333, 334, and 419) as ligands to the metals of the binuclear center. The loss of the heme a_3-specific resonance Raman bands is most easily explained by structural disruption of the heme crevice by each of these mutations, such that heme a_3 assumes multiple conformations. This would result in broadening and apparent loss of these resonance Raman modes even though heme a_3 is still present.

CONCLUSIONS

The results of these studies can be interpreted in terms of a structural model displayed as a helical wheel diagram in Fig. 4. The main points are summarized below.

(*i*) Substitutions for each of the totally conserved histidines in subunit I result in elimination of cytochrome *c* oxidase activity but do not prevent insertion of the polypeptide into the membrane or assembly of inactive oxidase species. These data are consistent with the six histidines being metal ligands. Since these histidines are located within putative transmembrane helices II, VI, VII, and X, these four helices must provide the framework for the catalytic core. The four helices are shown in projection in Fig. 4.

(*ii*) His-102 and His-421 are deduced to be the ligands for the six-coordinate heme *a* component of the oxidase, from the loss of the heme *a* spectrum in the mutant proteins and by elimination of the other conserved histidines because of their retention of distinctive heme *a* spectral characteristics. Hence, helices II and X must be adjacent to provide the ligands to this heme.

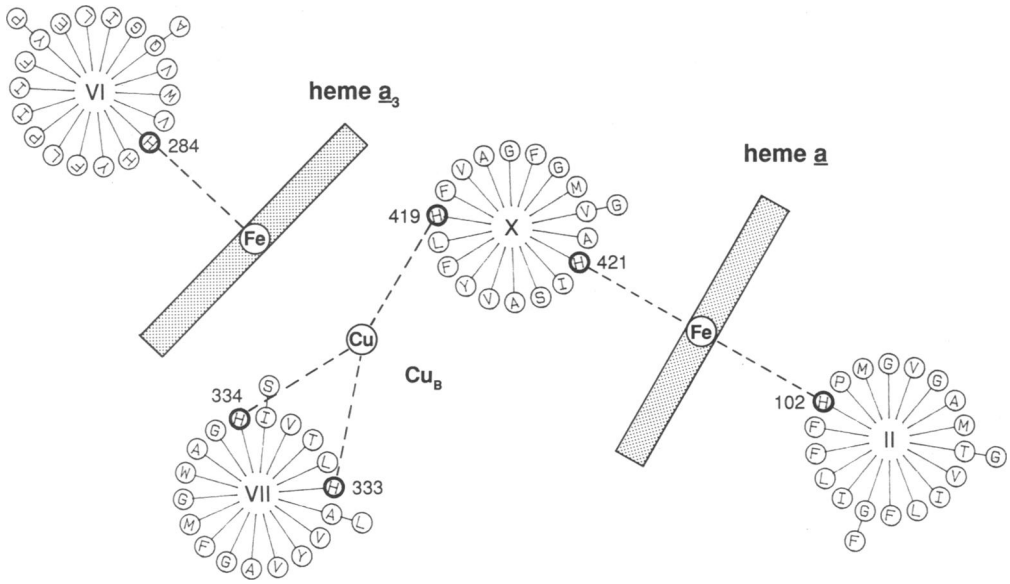

FIG. 4. A model of the ligation of heme *a*, heme a_3, and Cu_B by the six conserved histidines of subunit I. Helical wheel representations of helices II, VI, VII, and X are shown; the histidine ligands are in bold circles. The estimated length of the imidazole side chains is included in the broken lines representing the N_{His}–metal bonds. The heme a_3 iron to Cu_B distance is drawn as 5 Å, while the iron-to-iron distance of the two hemes is drawn as 15 Å.

(*iii*) Mutations at His-284, His-333, His-334, and His-419 all disrupt the binuclear center to some extent, consistent with these histidines being metal ligands to either Cu_B or heme a_3.

(*iv*) The His-333 → Asn mutant does not disrupt the specific resonance Raman features associated with heme a_3 and therefore His-333 cannot be the axial ligand of this heme. It must then be a Cu_B ligand.

(*v*) Since Cu_B is on the distal side of heme a_3 and within 3–5 Å of the iron (37, 38), it is difficult to assign His-334 as the heme a_3 axial ligand; this would place Cu_B on the wrong side of heme a_3. Hence, His-334 is also assigned as a Cu_B ligand. To accommodate adjacent histidines (333 and 334) as copper ligands, some disruption of the α-helical structure is expected, but this might be predicted in any case to permit a conformationally driven proton-conducting pathway to function in this region.

(*vi*) The data do not distinguish whether His-284 or His-419 is the ligand to heme a_3. Analysis of mutants in the structurally related *bo*-type oxidase from *E. coli* suggest that His-284 is a more likely choice (39, 40). However, these data are by no means definitive, and this must be considered the most speculative aspect of the model shown in Fig. 4. Having assigned His-284 as the heme a_3 axial ligand, we assign His-419 as the third histidine ligand to Cu_B.

The model shown in Fig. 4 is not intended to be definitive but is, rather, a working model with some speculative elements. Even if the ligand assignments are entirely correct, the placement of the four helices is not uniquely defined. The relationships of helices II, VII, and X are severely constrained by metal ligation, but the placement of helix VI is less constrained, even considering the estimated distance between the two heme irons (41). The placement chosen here is consistent with rapid electron transfer between heme *a* and the binuclear center (42) and with the proposal that Cu_B is the primary acceptor of electrons from heme *a* (43).

It is interesting to note that helix X contains ligands for both heme *a* (His-421) and Cu_B (His-419). It might be expected that alterations in either of these residues would influence both heme centers, since heme a_3 is close to Cu_B. Indeed, the resonance Raman spectrum of His-419 → Asn shows a shift of the 266 cm^{-1} band, which has been assigned to heme *a* (32). There is also an increase in the unassigned band at 376 cm^{-1}. These changes may indicate a slight alteration in the heme *a* environment. The structural link via helix X between the heme a_3–Cu_B center and heme *a* provides an attractive mechanism for conformational coupling between the metal centers of the oxidase (44) as well as negative cooperativity between heme *a* and Cu_B (43). Both phenomena may be critical to the proton-pumping activity of the enzyme.

This work was supported by grants from the National Institutes of Health (GM26916, to S.F.-M.; GM25480, to G.T.B.; HL16101, to R.B.G.; GM13047, to MMJT), the Human Frontier Science Program (to R.B.G.), and the Research Excellence Fund, State of Michigan (to S.F.-M. and J.P.H.).

1. Chan, S. I. & Li, P. M. (1990) *Biochemistry* **29**, 1–12.
2. Saraste, M. (1990) *Q. Rev. Biophys.* **23**, 331–336.
3. Wikström, M. (1977) *Nature (London)* **266**, 271–273.
4. Ludwig, B. (1987) *FEMS Microbiol. Rev.* **46**, 41–56.
5. Fee, J. A., Kuila, D., Mather, M. W. & Yoshida, T. (1986) *Biochim. Biophys. Acta* **853**, 153–185.
6. Paddock, M. L., Feher, G. & Okamura, M. Y. (1991) *Photosyn. Res.* **27**, 109–119.
7. Yun, C.-H., Crofts, A. R. & Gennis, R. B. (1991) *Biochemistry* **30**, 6747–6754.
8. Cao, J., Shapleigh, J., Gennis, R., Revzin, A. & Ferguson-Miller (1991) *Gene* **101**, 133–137.
9. Shapleigh, J. P. & Gennis, R. B. (1992) *Mol. Microbiol.* **6**, 635–642.
10. Raitio, M., Jalli, T. & Saraste, M. (1987) *EMBO J.* **6**, 2825–2833.
11. Holm, L., Saraste, M. & Wikström, M. (1987) *EMBO J.* **6**, 2819–2823.
12. Raitio, M., Pispa, J. M., Metso, T. & Saraste, M. (1990) *FEBS Lett.* **261**, 431–435.
13. Gabel, C. & Maier, R. J. (1990) *Nucleic Acids Res.* **18**, 6143.
14. Bott, M., Bolliger, M. & Hennecke, H. (1990) *Mol. Microbiol.* **4**, 2147–2157.
15. Gadsby, P. M. A. & Thomson, A. J. (1990) *J. Am. Chem. Soc.* **112**, 5003–5011.
16. Carter, K. & Palmer, G. (1982) *J. Biol. Chem.* **257**, 13507–13514.
17. Babcock, G. T., VanSteelandt, J., Palmer, G., Vickery, L. E. & Salmeen, I. (1979) in *Cytochrome Oxidase*, eds. King, T. E., Orii, Y., Chance, B. & Okunuki, K., (Elsevier/North Holland, Amsterdam), pp. 105–115.
18. Martin, C. T., Scholes, C. P. & Chan, S. I. (1985) *J. Biol. Chem.* **260**, 2857–2861.
19. Stevens, T. H. & Chan, S. I. (1981) *J. Biol. Chem.* **256**, 1069–1071.
20. Ogura, T., Hon-Nami, K., Oshima, T., Yoshikawa, S. & Kitigawa, T. (1983) *J. Am. Chem. Soc.* **105**, 7781–7782.
21. Cline, J., Reinhammar, B., Jensen, P., Venters, R. & Hoffman, B. M. (1983) *J. Biol. Chem.* **258**, 5124–5128.
22. Li, P. M., Gelles, J., Chan, S. I., Sullivan, R. J. & Scott, R. A. (1987) *Biochemistry* **26**, 2091–2095.
23. Vandeyar, M. A., Weiner, M. P., Hutton, C. J. & Batt, C. A. (1988) *Gene* **65**, 129–133.
24. Sanger, F., Nicklen, S. & Coulson, A. R. (1977) *Proc. Natl. Acad. Sci. USA* **74**, 5463–5467.
25. Keen, N. T., Tamaki, S., Kobayashi, D. & Trollinger, D. (1988) *Gene* **70**, 191–197.
26. Simon, R., Priefer, U. & Pühler, A. (1983) *Bio/Technology* **1**, 784–791.
27. Cohen-Bazire, G., Sistrom, W. R. & Stanier, R. Y. (1957) *J. Cell Comp. Physiol.* **49**, 25–68.
28. Berry, E. A. & Trumpower, B. L. (1987) *Anal. Biochem.* **161**, 1–15.
29. Vanneste, W. H. (1966) *Biochemistry* **65**, 838–848.
30. Wielburski, A. & Nelson, B. D. (1984) *FEBS Lett.* **177**, 291–294.
31. Fetter, J., Hosler, J. P., Shapleigh, J. P., Tecklenburg, M. M. J., Gennis, R. B., Babcock, G. T. & Ferguson-Miller, S. (1992) *Biophys. J.* **61**, A203 (abstr.).
32. Babcock, G. T. (1988) in *Biological Applications of Raman Spectroscopy*, ed. Spiro, T. G. (Wiley, New York), pp. 294–346.
33. Babcock, G. T., Callahan, P. M., Ondrias, M. R. & Salmeen, I. (1981) *Biochemistry* **20**, 959–966.
34. Ching, Y.-C., Argade, P. V. & Rousseau, D. L. (1985) *Biochemistry* **24**, 4938–4946.
35. Woodruff, W. H., Dallinger, R. F., Antalis, T. M. & Palmer, G. (1981) *Biochemistry* **20**, 1332–1340.
36. Nagai, M., Yoneyama, Y. & Kitagawa, T. (1991) *Biochemistry* **30**, 6495–6503.
37. Scott, R. A., Schwartz, J. R. & Cramer, S. (1986) *Biochemistry* **25**, 5546–5555.
38. Powers, L., Chance, B., Ching, Y. & Angiolillo, P. (1981) *Biophys. J.* **34**, 465–498.
39. Minagawa, J., Mogi, T., Gennis, R. B. & Anraku, Y. (1992) *J. Biol. Chem.* **267**, 2096–2104.
40. Lemieux, L. J., Calhoun, M. W., Thomas, J. W., Ingledew, W. J. & Gennis, R. B. (1992) *J. Biol. Chem.* **267**, 2105–2113.
41. Ohnishi, T., LoBrutto, R., Salerno, J. C., Bruckner, R. C. & Frey, T. G. (1982) *J. Biol. Chem.* **257**, 14821–14825.
42. Oliveberg, M. & Malmstrom, B. G. (1991) *Biochemistry* **30**, 7053–7057.
43. Babcock, G. T. & Wikström, M. (1992) *Nature (London)*, in press.
44. Copeland, R. A. (1991) *Proc. Natl. Acad. Sci. USA* **88**, 7281–7283.